



Ras- and PI3K-dependent breast tumorigenesis in mice and humans requires focal adhesion kinase signaling

Yuliya Pylayeva,^{1,2} Kelly M. Gillen,^{1,2} William Gerald,³ Hilary E. Beggs,^{4,5} Louis F. Reichardt,⁵ and Filippo G. Giancotti¹

¹Cell Biology Program, Memorial Sloan-Kettering Cancer Center (MSKCC), New York, New York, USA.

²Sloan-Kettering Division, Weill Graduate School of Medical Sciences, Cornell University, New York, New York, USA.

³Human Oncology and Pathogenesis Program and Department of Pathology, MSKCC, New York, New York, USA.

⁴Department of Ophthalmology and ⁵Department of Physiology, UCSF, San Francisco, California, USA.

Cancer cells require sustained oncogenic signaling in order to maintain their malignant properties. It is, however, unclear whether they possess other dependencies that can be exploited therapeutically. We report here that in a large fraction of human breast cancers, the gene encoding focal adhesion kinase (FAK), a core component of integrin signaling, was amplified and FAK mRNA was overexpressed. A mammary gland-specific deletion of *Fak* in mice did not seem to affect normal mammary epithelial cells, and these mice were protected from tumors initiated by the polyoma middle T oncoprotein (PyMT), which activates Ras and PI3K. FAK-deficient PyMT-transformed cells displayed both growth arrest and apoptosis, as well as diminished invasive and metastatic capacity. Upon silencing of *Fak*, mouse mammary tumor cells transformed by activated Ras became senescent and lost their invasive ability. Further, *Neu*-transformed cells also underwent growth arrest and apoptosis if integrin $\beta 4$ -dependent signaling was simultaneously inactivated. Human breast cancer cells carrying oncogenic mutations that activate Ras or PI3K signaling displayed similar responses upon silencing of FAK. Mechanistic studies indicated that FAK sustains tumorigenesis by promoting Src-mediated phosphorylation of p130^{Cas}. These results suggest that FAK supports Ras- and PI3K-dependent mammary tumor initiation, maintenance, and progression to metastasis by orchestrating multiple core cellular functions, including proliferation, survival, and avoidance of senescence.

Introduction

Cancer cells require sustained oncogenic signaling in order to thrive (1). A large fraction of breast tumors carry oncogenic mutations that cause hyperactivation of the Raf/ERK cascade (20%–25% *HER2*, 5% *KRAS*, 2% *BRAF*, 1% *HRAS*, 1% *NRAS*) or of PI3K signaling (20%–25% *HER2*, 26% *PIK3CA*, 8% *AKT1*, 5% *PTEN*) (2–4). Furthermore, introduction of oncogenic *HRAS* or *PIK3CA* in combination with the SV-40 T antigen and hTERT is sufficient for tumorigenic conversion of human mammary epithelial cells (5, 6). Hence, many therapies under development for tumors of the breast and other tissues aim to interrupt Ras or PI3K signaling.

The integrin adhesion receptors associate with receptor tyrosine kinases to regulate cell survival, mitogenesis, and cell migration (7). Changes in the level of expression or activation of individual integrins may thus enhance transmission of pro-growth and pro-migratory signals in cancer cells. In accordance with this model, it has been shown that the $\beta 4$ integrin combines with an activated, oncogenic version of ErbB2 to amplify mitogenic and invasive signaling during mammary tumorigenesis (8). However, most oncogenic mutations deregulate signaling components, such as Ras and PI3K, which function downstream of integrins and receptor tyrosine kinases. It has been argued that these prevalent mutations alle-

viate the requirement for integrin signaling, enabling tumor cells to survive and proliferate even if denied anchorage to the matrix (9). In agreement with this model, available evidence implicates integrin signaling in tumor progression rather than tumor initiation or maintenance (10, 11). It has been reported that deletion of all $\beta 1$ integrins, of which several are expressed in mammary epithelial cells, suppresses polyoma middle T-mediated (PyMT-mediated) mammary tumorigenesis (12), but this result neither distinguishes between a requirement for integrin-mediated adhesion or signaling nor identifies which integrin signaling pathway, among the many known, would be necessary for tumor initiation.

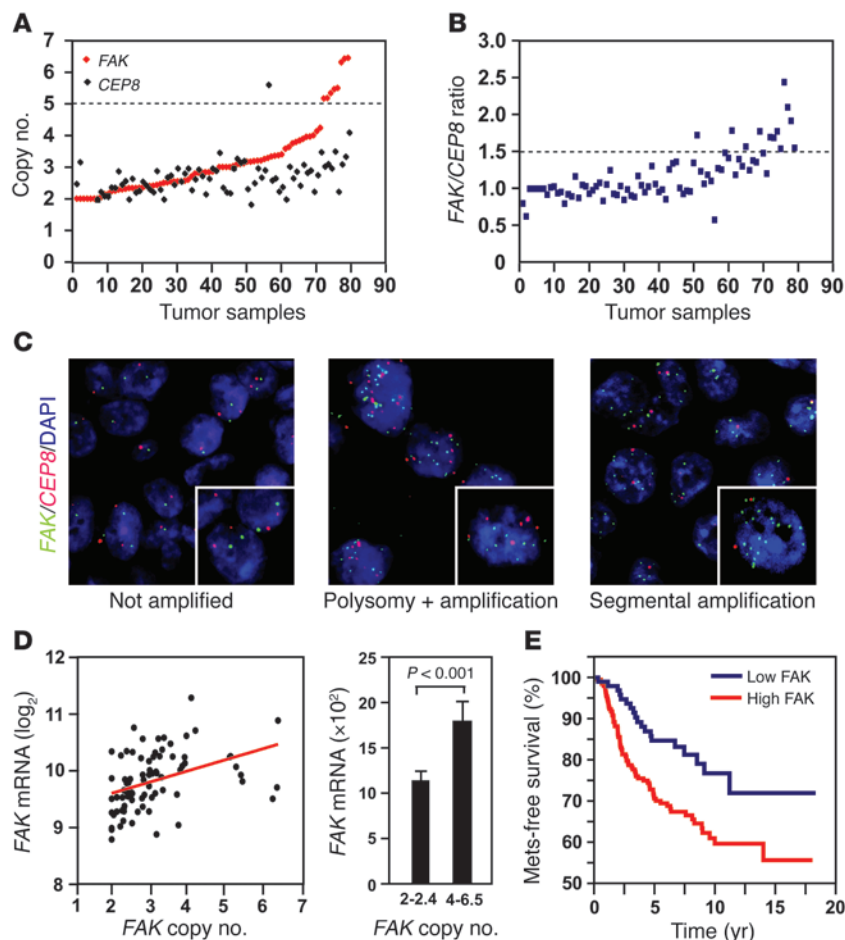
The non-receptor tyrosine kinase focal adhesion kinase (FAK) is a major mediator of integrin signaling (13). Engagement of $\beta 1$ and αv – but not $\beta 4$ – integrins induces FAK localization to matrix adhesions and activation. Upon autophosphorylation at Tyr397, FAK combines with Src or another Src family kinase (SFK). The SFK in turn phosphorylates FAK and FAK-associated focal adhesion proteins, such as p130^{Cas}, paxillin, and p190-Rho-GEF, on tyrosine residues. In addition, FAK can combine with PI3K and Grb7 and activate the tyrosine kinase Etk/BMX. Through this plethora of effectors, FAK regulates focal adhesion dynamics during cell migration and activates prosurvival and mitogenic signaling pathways (14).

Genetic studies have indicated that FAK regulates cell survival and cell proliferation only in selected cell types. FAK-null fibroblasts and keratinocytes do not display reduced proliferation in vitro (15, 16), and loss of FAK results in apoptosis in embryonic fibroblasts and endothelial cells but not in meningeal fibroblasts

Conflict of interest: The authors have declared that no conflict of interest exists.

Nonstandard abbreviations used: FAK, focal adhesion kinase; MIN, mammary intraepithelial neoplasia; PyMT, polyoma middle T; SAHF, senescence-associated heterochromatic foci; SFK, Src family kinase; SFM, serum-free medium.

Citation for this article: *J. Clin. Invest.* 119:252–266 (2009). doi:10.1172/JCI37160.

**Figure 1**

Amplification of *FAK* in human breast cancer. (A–D) Primary tumors ($n = 79$) from the MSKCC breast tumor collection were subjected to FISH and DNA microarray analysis. (A) Average number of copies of *FAK* and *CEP8*. (B) *FAK/CEP8* ratio in the same tumors. Tumors are ordered as in A. (C) Images from representative cases: not amplified (left), polysomy and amplification (middle), and amplification (right). Original magnification, $\times 630$; $\times 945$ (insets). (D) Correlation between *FAK* copy number and mRNA expression. $r^2 = 0.16$; $P = 0.0002$. (E) Kaplan-Meier analysis of metastasis-free survival in the NKI cohort. $n = 295$; $P = 0.0062$.

(15, 17, 18). However, it is unclear whether the differential effects that loss of FAK exerts in different cell types reflect genuine cell type-specific roles of the kinase or selective compensatory upregulation of the FAK-related kinase PYK2 (19, 20). A further complication arises from the recent realization that FAK also exerts kinase-independent functions (21, 22).

Several observations suggest that FAK is not required for neoplastic transformation but promotes cancer cell invasion (14). For example, v-Src can transform FAK-null fibroblasts efficiently, but FAK kinase activity is required for invasion through Matrigel in vitro and metastasis in nude mice (23, 24). Furthermore, deletion of FAK inhibits conversion of papilloma to carcinoma in the TPA-DMBA skin carcinogenesis model (25) and progression to adenocarcinoma in the PyMT model of mammary tumorigenesis (26). Finally, knockdown of FAK inhibits the ability of SK-Br3 and T47D human breast cancer cells to invade in vitro (27) and that of 4T1 mouse mammary carcinoma cells to metastasize in vivo (28). It is currently unknown whether FAK is required for tumor initiation or maintenance in the breast or other organs.

Pathological studies suggest that a large fraction of breast cancers express elevated levels of FAK (29, 30). Here we have used genomic analysis of primary tumor specimens and whole animal and cell culture models to examine the role of FAK in breast cancer. We show that the gene encoding FAK is frequently amplified in human breast cancer. We demonstrate that FAK is required for Ras- and PI3K-dependent transformation of the mammary gland.

Finally, we provide evidence that FAK orchestrates a wide range of cellular functions necessary for tumor maintenance, including survival, proliferation, and suppression of senescence.

Results

FAK is amplified and overexpressed in a large fraction of human breast cancers. The gene encoding FAK (*PTK2*; herein referred to as *FAK*) resides on the distal end of the long arm of chromosome 8 at q24, within a genomic region that contains the oncogene *MYC* and is frequently amplified in breast cancer (31). A recent array comparative genomic hybridization (CGH) analysis has suggested that 8q24 contains 2 distinct amplicons, q24.11-13, which includes *MYC*, and q24.3, which includes *FAK* (32). To directly address whether *FAK* is amplified in breast cancer, we conducted 2-color FISH on tissue microarrays containing 79 primary breast tumors collected at MSKCC. Confocal analysis revealed that a large fraction of these tumors displayed an elevated *FAK* copy number. Approximately 50% of the samples contained tumor cells with an average of more than 3 copies of *FAK* and about 10% displayed high-level amplification (*FAK* copy number, > 5) (Figure 1A). The probe hybridizing with centromere 8 (*CEP8*) frequently detected modest gains (*CEP8* copy number, 2.5–3) (Figure 1A). However, the samples exhibiting high-level amplification of *FAK* did not show a corresponding increase in *CEP8* copy number, consistent with segmental amplification of *FAK* (*FAK/CEP8* ratio, > 1.5) (Figure 1, A and B). *FAK* copy numbers appeared to vary among nuclei of tumor cells from the



Table 1
Multivariate Cox regression analysis on the NKI cohort of breast cancer patients

Variable	P	Hazard ratio	CI
Elevated FAK	0.035	1.75	1.04–2.93
Size	0.003	2.03	1.28–3.22
LN+	0.21	0.76	0.49–1.17
ER+	0.57	0.87	0.53–1.42
III PD	0.4	1.24	0.75–2.03
III WD	0.02	0.42	0.2–0.89
HER2+	0.035	1.73	1.04–2.86

III PD, poorly differentiated; III WD, well differentiated.

same sample (Figure 1C), with individual nuclei displaying up to 23 copies of FAK (Supplemental Figure 1A; supplemental material available online with this article; doi:10.1172/JCI37160DS1).

To examine whether amplification of *FAK* correlates with expression of the corresponding mRNA, we examined the transcriptomic profiles of the same breast cancer dataset. Increased *FAK* copy number and *FAK/CEP8* ratio correlated positively with expression of *FAK* (Figure 1D and Supplemental Figure 1B). In contrast, *FAK/CEP8* ratio did not correlate with expression of *MYC* (Supplemental Figure 1C). These results indicate that *FAK* is amplified and overexpressed in a large fraction of primary human breast cancers.

High levels of FAK correlate with progression to metastasis in human breast cancer. To examine whether high levels of FAK identify breast cancers with a poor prognosis, we analyzed the Netherlands Cancer Institute (NKI) DNA microarray dataset, which contains the gene expression profiles of stage I or II primary tumors from 295 patients and has been annotated with extensive clinical follow-up data (33). In contrast, our MSKCC dataset comprises more advanced tumors (data not shown). The NKI samples were divided into 2 groups depending on the level of expression of FAK mRNA (top two-thirds with high or medium Z score and bottom third with low Z score) (Supplemental Figure 2A). Primary tumors with high levels of FAK displayed a size distribution similar to those with low levels of FAK (Supplemental Figure 2B) and were not characterized by a specific histological grade (Supplemental Figure 2C), ER status (Supplemental Figure 2D), or transcriptomic subtype (Supplemental Figure 2E). Kaplan-Meier analysis revealed that the patients with high levels of *FAK* mRNA had a significantly shorter metastasis-free survival than those with low levels (Figure 1E). In addition, multivariate Cox regression showed that elevated expression of *FAK* correlates with poor survival independent of other commonly used clinical parameters and provided evidence that elevated FAK is a better predictor of poor outcome than lymph node involvement, ER negativity, or poor differentiation (Table 1). In contrast, high levels of *MYC* mRNA did not correlate with poor prognosis in the same dataset (Supplemental Figure 3). Taken together, these results suggest that *FAK* amplification and overexpression contribute to human breast cancer malignancy.

Postnatal deletion of FAK does not impair mammary gland development. To examine the effect of loss of *FAK* on mammary tumorigenesis, we generated mice carrying a mammary gland-specific deletion of *FAK* by crossing *FAK^{fl/fl}* mice (17) to *MMTV-Cre* mice (line D; ref. 34). Preliminary experiments had demonstrated efficient deletion of the *loxP*-flanked transcription stop site of the *Rosa26* allele and, thereby, expression of β -galactosidase in a majority of mammary

epithelial cells (estimated as 96.4%) in *MMTV-Cre;Rosa26* compound mice (Supplemental Figure 4A), indicating that the *MMTV-Cre* line D transgene directs efficient deletion in mammary epithelium. As anticipated, however, a small proportion of ductal and luminal cells did not undergo Cre-mediated deletion of the reporter stop site, presumably because of inefficient expression of the Cre transgene.

Upon crossing *FAK^{fl/fl}* mice to *MMTV-Cre* mice, we sought to document a loss of FAK expression in *MMTV-Cre;FAK^{fl/fl}* mice. Since FAK is expressed at low levels in mammary epithelial cells in vivo (see Supplemental Figure 5, A–C), we first isolated primary mammary epithelial cells from *MMTV-Cre;FAK^{fl/fl}* mice and control mice and subjected them to immunoblotting. Whereas cells from control mice were found to express substantial amounts of FAK, consistent with the hypothesis that FAK expression is upregulated in culture, cells from *MMTV-Cre;FAK^{fl/fl}* mice did not express FAK (Supplemental Figure 4B). Deletion of FAK did not result in increased expression or activation of the FAK-related kinase PYK2 (Supplemental Figure 4B), in agreement with the observation that PYK2 does not localize to focal adhesions and therefore does not necessarily compensate for loss of FAK in integrin signaling (35). In addition, mammary epithelial cells did not express detectable levels of the FAK-related non-kinase (FRNK), and deletion of FAK did not lead to its induction (Supplemental Figure 4C and data not shown), consistent with observations from conditional deletion of *FAK* in the neuronal cortex (17). Finally, we crossed *MMTV-Cre;FAK^{fl/fl}* mice to *Rosa26* mice. Combined X-gal and anti-FAK staining indicated that expression of Cre, and thereby β -galactosidase, correlated with loss of FAK in most mammary epithelial cells of compound mice (Supplemental Figure 4D). These results indicate that expression of *MMTV-Cre* causes efficient deletion of *FAK* in mammary epithelium.

Whole mount analysis of ductal branching and outgrowth indicated that *MMTV-Cre;FAK^{fl/fl}* female mice undergo normal mammary gland morphogenesis (Supplemental Figure 4E). Their lobuloalveolar units are histologically indistinguishable from those of wild-type mice. Furthermore, these mice are able to nurse their progeny effectively. Finally, breeding to *Rosa26* mice indicated that *FAK*-null mammary epithelial cells contribute efficiently to ductal branching and outgrowth (Supplemental Figure 4F). Since *MMTV-Cre* is expressed from postnatal day 22 in line D mice, we conclude that loss of FAK at this developmental stage does not cause obvious defects in mammary gland development. In apparent contrast, deletion of *FAK* at E12.5 using the *MMTV-Cre* line F causes a delay in branching morphogenesis during puberty and a defect in luminal cell proliferation and differentiation during pregnancy, suggesting that deletion of FAK at this earlier embryonic stage affects subsequent development of the mammary gland (36).

Deletion of FAK suppresses PyMT-induced mammary tumorigenesis. To examine the role of FAK in mammary tumorigenesis, we introduced conditional deletion of *FAK* into *MMTV-PyMT* mice, which undergo multistep progression to mammary carcinoma following PyMT-mediated activation of Ras and PI3K (37). Immunohistochemical staining and in situ hybridization showed that the levels of FAK and its autophosphorylation at Y397 are not significantly elevated in hyperplastic lesions, which convert into neoplastic lesions at a very low frequency (37, 38), but they increase substantially in mammary intraepithelial neoplasia (MIN) lesions (Supplemental Figure 5, A–C), the first morphologically identifiable neoplastic lesions in this model (39), consistent with a potential role of FAK in Ras- and PI3K-mediated mammary tumorigenesis.

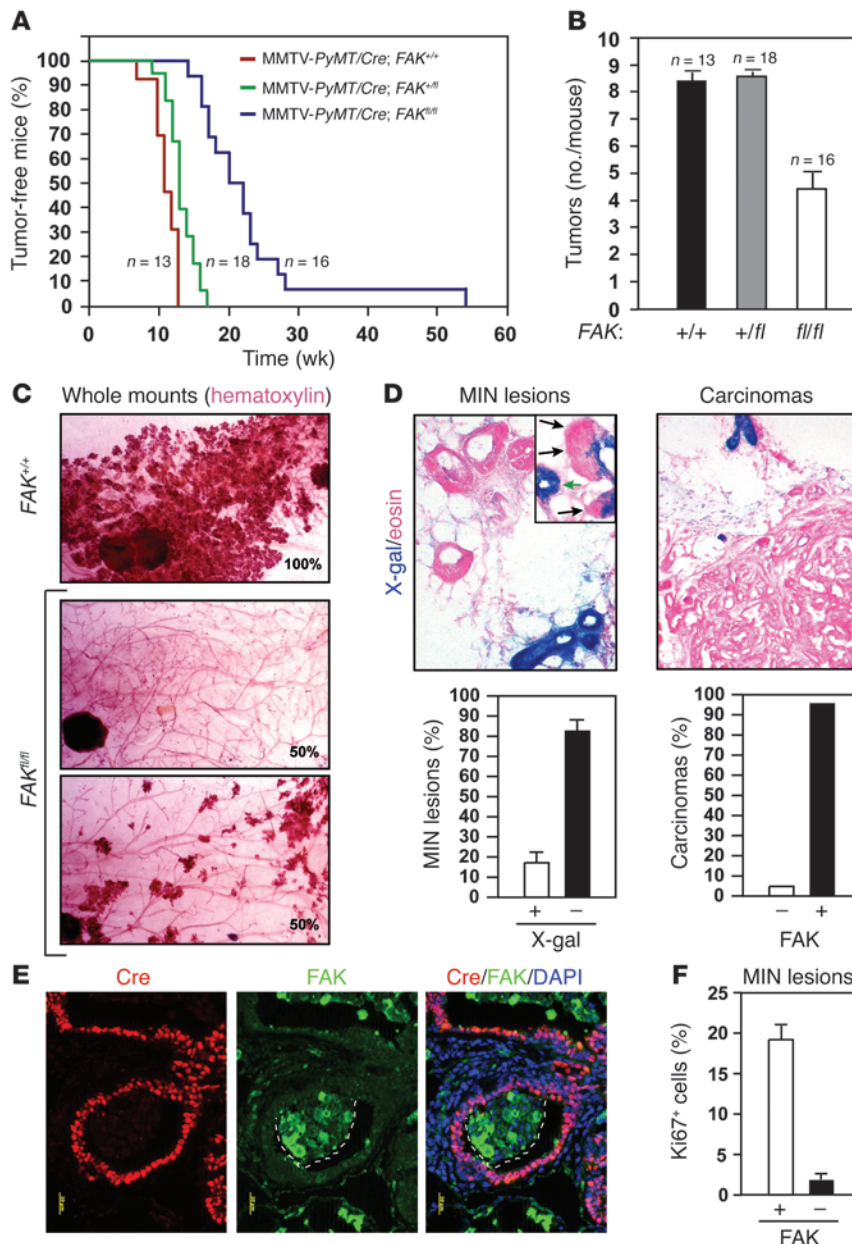


Figure 2

Conditional deletion of *FAK* suppresses mammary tumorigenesis in MMTV-*PyMT* mice. (A) Kaplan-Meier analysis of tumor onset in mice of the indicated genotypes. $P < 0.0001$, *FAK*^{+/+} or *FAK*^{+/-} versus *FAK*^{-/-}. (B) Mean number of tumors per mouse (\pm SEM) in MMTV-*PyMT* mice of the indicated genotype at the time of sacrifice. $P < 0.0001$, *FAK*^{+/+} or *FAK*^{+/-} versus *FAK*^{-/-}. (C) Whole mounts of mammary glands from 12-week-old MMTV-*PyMT* mice of the indicated genotype were stained with hematoxylin. Percentages indicate the frequency of observed phenotypes ($n = 8$ per genotype). Original magnification, $\times 20$. (D) Mammary glands from 6-month-old MMTV-*PyMT*/Cre;*FAK*^{-/-};R26R mice were subjected to β -galactosidase staining and counterstaining with eosin. Insert in top left panel shows early MIN lesions budding out of normal ducts (black arrows) and an unaffected duct (green arrow). Graph on the bottom left indicates the percentage of X-gal-positive and -negative MIN lesions (error bars denote SEM); $P = 2.8 \times 10^{-15}$. Graph on the bottom right indicates the percentage of FAK-null and FAK-expressing adenocarcinomas. Original magnification, $\times 200$ (left); $\times 400$ (inset); $\times 100$ (right). (E) FAK and Cre staining on early MIN lesions from MMTV-*PyMT*/MMTV-Cre;*FAK*^{-/-} mice. The dotted outline indicates a FAK-positive early intraductal lesion. (F) Percentage of Ki67-positive tumor cells (error bars denote SEM) in FAK-expressing and FAK-null MIN lesions; $P = 3.4 \times 10^{-11}$.

MMTV-*PyMT*/MMTV-Cre;*FAK*^{1/1} mice developed palpable tumors significantly later than MMTV-*PyMT*/MMTV-Cre;*FAK*^{+/+} mice (Figure 2A). Median tumor onset was delayed by 11 weeks in *FAK* mutant mice. Moreover, these mice developed significantly fewer tumors as compared with control mice (Figure 2B). Finally, the mammary glands of MMTV-*PyMT*/MMTV-Cre;*FAK*^{1/1} mice exhibited a drastic reduction in MIN lesions at 12 weeks of age as compared with those of control mice, which were completely replaced by MIN lesions and individual large tumors at this stage (Figure 2C). These observations indicate that deletion of *FAK* inhibits PyMT-mediated mammary tumorigenesis.

Strikingly, immunoblotting and in situ hybridization analyses indicated that virtually all tumors arising in MMTV-*PyMT*/MMTV-Cre;*FAK*^{1/1} mice (43 of 45; 95.5%) expressed *FAK* (Supplemental Figure 6), consistent with the hypothesis that they had originated from the minority of mammary epithelial cells that had not under-

gone Cre-mediated recombination of *FAK*. Indeed, upon breeding MMTV-*PyMT*/MMTV-Cre;*FAK*^{1/1} mice to *Rosa26* mice, we found that most MIN lesions and tumors arising in *FAK* mutant mice carrying the reporter did not express β -galactosidase, whereas the majority of cells in normal ducts and lobules expressed the enzyme (Figure 2D). Interestingly, even incipient MIN lesions budding out of otherwise normal ducts comprised cells that did not express β -galactosidase (Figure 2D; inset in upper left panel). Immunohistochemical staining confirmed loss of Cre and expression of *FAK* in these early lesions (Figure 2E; early intraductal lesion). These results suggest that *FAK* is required for tumor initiation in this mouse model.

After the studies described in this article were completed, Lahlou et al. reported that conditional deletion of *FAK* using a less-efficient MMTV-Cre line (64.3% excision) inhibits tumor progression but not initiation in the PyMT model (26). They reached this conclusion because they were able to detect hyperplasias as well as adenomas,

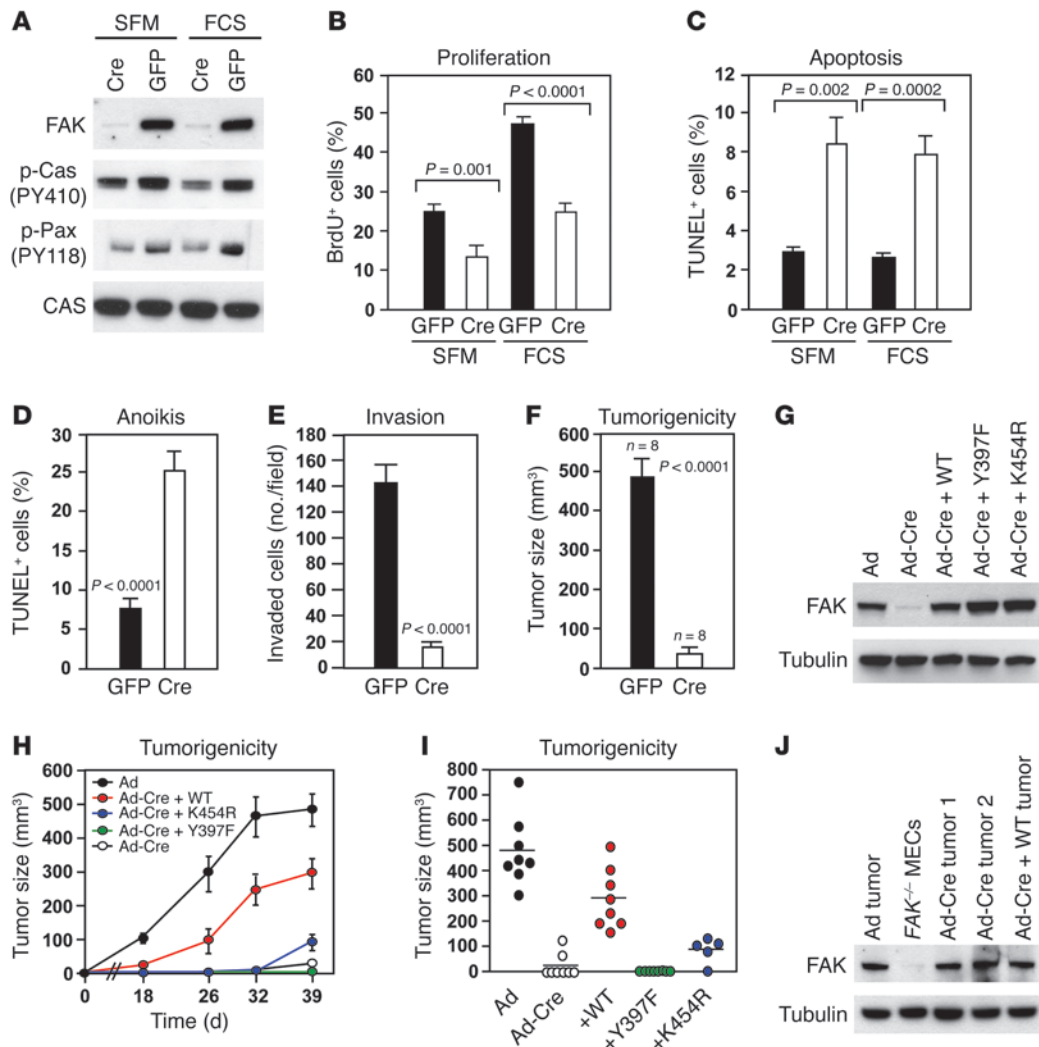


Figure 3

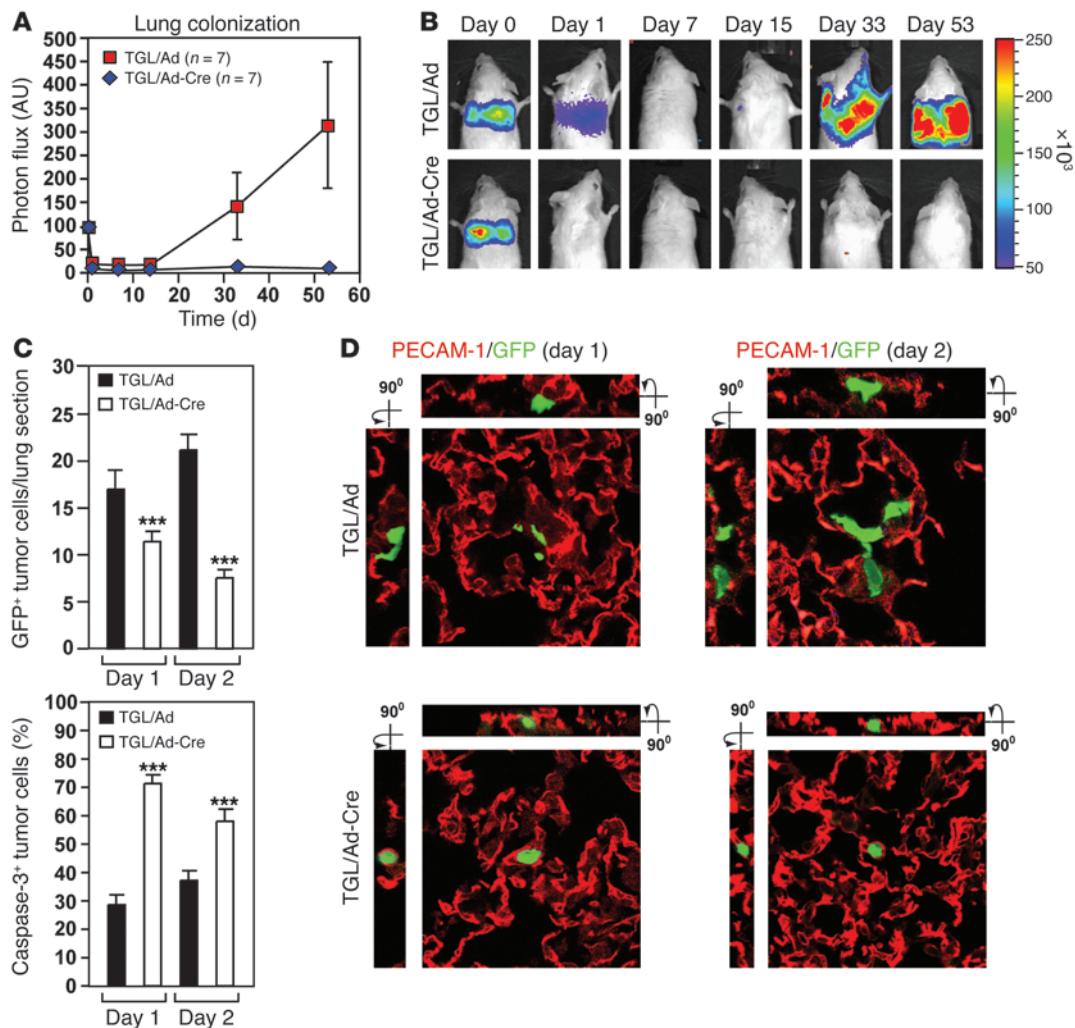
Deletion of *FAK* inhibits PyMT-transformed mammary tumor cells. (A–F) Primary tumor cells from MMTV-PyMT;FAK^{fl/fl} mice were transduced with adeno-GFP or adeno-Cre, cultured in SFM or complete medium (FCS), and subjected to immunoblotting (A); cultured on collagen I, starved for 24 hours, and incubated in the presence of BrdU in complete medium for 24 hours (B); plated on collagen I and subjected to TUNEL assay (C); suspended in complete medium containing 0.5% methylcellulose and 1% BSA for 8 hours at 37°C and subjected to TUNEL assay (D); subjected to Matrigel invasion assay for 8 hours (E); or injected at 2 × 10⁵ in the mammary fat pads of NOD/SCID mice to evaluate tumorigenicity (F). The graphs indicate mean values ± SEM. (G–J). Primary tumor cells from MMTV-PyMT;FAK^{fl/fl} mice were transduced with empty retroviral vector or the indicated constructs, infected with adeno-GFP or adeno-Cre, subjected to immunoblotting (G), and injected orthotopically into NOD/SCID mice (H–J). (H) Mean tumor volumes (±SEM) over time (n = 4 per group). (I) Size of individual tumors and mean size in each class at day 39. (J) Tumor lysates were subjected to immunoblotting. FAK^{-/-} mammary epithelial cells were used as control. Ad tumor, adeno-GFP tumor. Error bars denote SEM.

but not carcinomas, comprising cells that had undergone excision of *FAK* in their MMTV-PyMT;MMTV-Cre;FAK^{fl/fl} mice. However, since they did not estimate the percentage of MIN lesions or even adenomas developing in the absence of *FAK* in their mice, they may have overlooked an effect of deletion of *FAK* on tumor initiation.

Since the MINs are the earliest morphologically recognizable neoplastic lesions, we reasoned that it was important to estimate what percentage of these lesions originated from cells that had escaped Cre-mediated recombination of *FAK* in our mice. X-gal staining indicated that more than 80% of the MIN lesions arising in MMTV-PyMT;MMTV-Cre;FAK^{fl/fl} mice did not express β-galactosidase, indicating that they were derived from cells that had not undergone Cre-mediated recombination of *FAK* (Figure 2D, lower left). MIN

lesions that were derived from unrecombined cells and therefore expressed *FAK* had a proliferative index much higher than that of those few that had undergone successful recombination and lacked *FAK* expression (Figure 2F and Supplemental Figure 7). However, both types of lesions had low apoptotic indices (data not shown). These results provide evidence that *FAK* is required for efficient tumor initiation in the PyMT model. The observation that the few MIN lesions that arise in the absence of *FAK* display a proliferative defect and do not progress to adenocarcinoma suggests that *FAK* is also required for tumor maintenance and progression.

Inactivation of FAK compromises the tumorigenic potential of PyMT-transformed cells. To examine the mechanism through which *FAK* promotes PyMT-dependent mammary tumorigenesis, we infected

**Figure 4**

Deletion of *FAK* suppresses metastasis to the lung. (A) Tumor cells from *MMTV-PyMT;FAK^{fl/fl}* mice were transduced with adeno-GFP (Ad) or adeno-Cre (Ad-Cre) and TGL, injected in the tail vein of NOD/SCID mice, and subjected to bioluminescence imaging. The graph shows the normalized photon flux in arbitrary units (\pm SEM); $P = 0.039$. (B) Representative images of mice injected with tumor cells transduced with the indicated viruses. Scale indicates the dynamic range of luminescent signal. (C) Quantification of GFP⁺ tumor cells present on lung sections at days 1 and 2 after tail vein injection (top). The percentage of GFP⁺ tumor cells undergoing apoptosis was estimated by staining with antibodies against cleaved caspase-3 (bottom). *** $P < 0.001$; $n = 4$ per group. Error bars denote SEM. (D) Lung sections from mice injected with tumor cells transduced with the indicated viruses were stained with anti-PECAM-1 (red) and subjected to confocal analysis. Panels show representative images at days 1 and 2. Original magnification, $\times 630$.

tumor cells derived from *PyMT;FAK^{fl/fl}* mice with an adenovirus encoding Cre. As anticipated, acute loss of FAK caused decreased phosphorylation of p130^{Cas} at Y410 and paxillin at Y118 (Figure 3A). It did not, however, completely suppress these phosphorylation events, presumably because SFKs can phosphorylate the cytoplasmic pool of p130^{Cas} and paxillin in the absence of FAK. Deletion of FAK inhibited tumor cell proliferation to a significant extent, both in serum-free medium (SFM) and in the presence of serum (Figure 3B). In addition, although it induced only a small fraction of tumor cells growing on collagen I to undergo apoptosis, in the absence or in the presence of serum (Figure 3C), it sensitized a larger fraction of them to anoikis, i.e., death upon detachment from the matrix in the presence of serum (Figure 3D). Finally, deletion of FAK almost completely inhibited the ability of

tumor cells to invade through Matrigel in vitro (Figure 3E). These results suggest that FAK promotes mammary tumor cell survival, proliferation, and invasion.

To examine the effect of deletion of FAK on tumorigenic potential, FAK-deficient and control *PyMT*-transformed cells were injected in the mammary fat pad of NOD/SCID mice. As shown in Figure 3F, FAK-deficient cells did not give rise to sizeable tumors in 1 month, whereas control cells gave rise to large tumors within the same time frame. These observations suggest that expression of FAK is required to maintain the oncogenic potential of *PyMT*-transformed cells.

To examine the mechanism through which FAK promotes *PyMT* mammary tumorigenesis, FAK-deficient mammary tumor cells were reconstituted with wild-type FAK; FAK-Y397F, which cannot combine with SFKs, PI3K, or Grb7; or FAK-K454R, which lacks

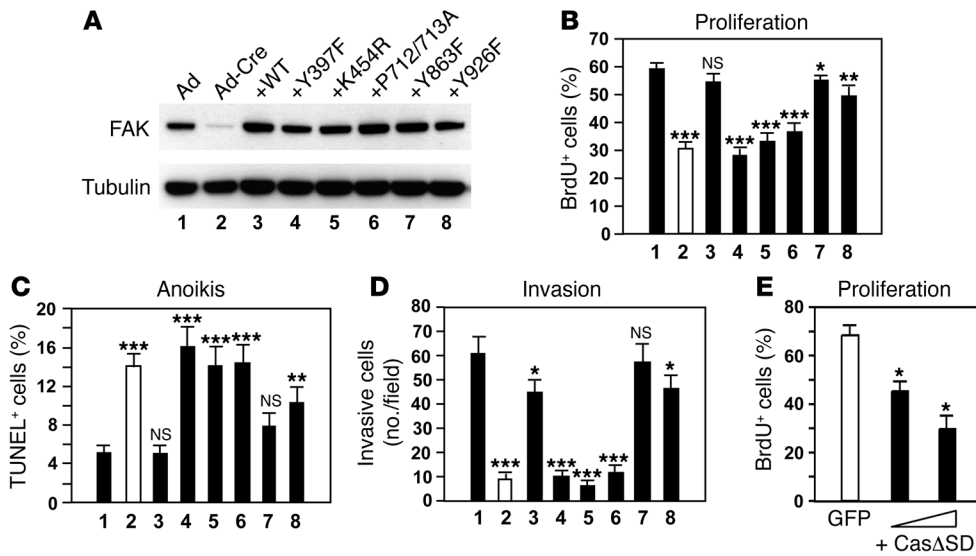


Figure 5

FAK kinase activity and Cas-binding motif of FAK promote mammary tumorigenesis. (A–D) Primary tumor cells from MMTV-PyMT;FAK^{fl/fl} mice were transduced with empty retrovirus or the indicated FAK constructs, infected with adeno-GFP or adeno-Cre, and subjected to immunoblotting (A); synchronized in G₀ and subjected to BrdU incorporation assay (B); cultured in suspension for 8 hours and subjected to TUNEL assay (C); or subjected to Matrigel invasion assay for 8 hours (D). The graph in D indicates the mean number of invasive cells (±SEM) per microscopic field. *P < 0.05, **P < 0.01, ***P < 0.001 compared with adeno-GFP; n = 3. PyMT FAK-proficient cells were transfected with either GFP or 1 or 2 μg of CasΔSD constructs, synchronized in G₀, and subjected to BrdU incorporation assay (E). The graph depicts percentages of GFP+BrdU⁺ cells (±SEM).

kinase activity (Figure 3G). As anticipated, FAK-deficient cells had a low tumorigenic potential (Figure 3, H and I). The only 2 small tumors that were generated by these cells expressed FAK and therefore arose from cells that had not been infected with adenoviral Cre (Figure 3, I and J). Reintroduction of wild-type FAK rescued mammary tumorigenesis to a large extent (Figure 3, H and I). The delay in tumor growth in this group of mice might be due to incomplete infection and thereby nonuniform reconstitution of the cells with FAK. By contrast, FAK-K454R, which is kinase-dead, did not rescue mammary tumorigenesis, suggesting that FAK kinase activity is required for this process. Reintroduction of FAK-Y397F was similarly ineffective, suggesting that FAK's autophosphorylation at Y397, which mediates interaction with SFKs, PI3K, and Grb7, is necessary for mammary tumorigenesis (Figure 3, H and I). These results implicate FAK's kinase activity and autophosphorylation at Y397 in mammary tumorigenesis.

Loss of FAK inhibits tumor cell survival in the bloodstream and homing to the lung. The effect of loss of FAK on tumor invasion and metastasis was examined using lung colonization assays. Mammary tumor cells from PyMT;FAK^{fl/fl} mice were infected with a retrovirus directing the expression of eGFP-TK-Luc from a single open reading frame (40) and then with an adeno-Cre or a control virus. The cells were then injected intravenously into NOD/SCID mice. Bioluminescent imaging revealed that control and FAK-null cells were immediately retained in the lungs with similar efficiency (Figure 4, A and B, day 0). However, 24 hours later, most of the FAK-null cells had disappeared from the lungs, whereas a significantly greater fraction of control cells remained in this organ (Figure 4B, day 1, and Figure C). Whereas mice injected with control cells developed large metastases by day 33, mice injected with FAK-null cells did

not develop detectable lung metastases over a 53-day period (Figure 4, A and B), suggesting that FAK promotes tumor cell retention in the microvascular compartment of the lung, extravasation, or outgrowth in the parenchyma of the organ.

To examine these possibilities, we performed confocal imaging on lung sections stained with anti-PECAM-1 (Figure 4D). In agreement with the results of bioluminescence imaging, we detected fewer GFP-positive cells on sections from mice injected with FAK-null cells than in those from mice injected with control cells at days 1 and 2 (Figure 4C, top), suggesting that FAK promotes tumor cell survival upon arrest in the capillary bed of the lung. In fact, anti-caspase-3 staining indicated that, upon arrest in the lung, FAK-deficient tumor cells underwent apoptosis more frequently than control cells (Figure 4C, bottom, and Supplemental Figure 8). Nev-

ertheless, a substantial proportion of FAK-null cells remained viable. To examine the fate of these cells, we performed confocal imaging with 3D reconstruction on lung sections stained with anti-PECAM-1. As shown in Figure 4D, control cells expressing FAK began to extravasate at day 1 by projecting lamellipodia across endothelial cell junctions and completed this process by day 2. Following extravasation, the FAK-positive cells spread extensively in the interstitial matrix of the lung, acquiring a distinctive morphology. Notably, all of the FAK-null tumor cells that were retained in the capillary bed of the lung displayed a round morphology and did not project lamellipodial extensions across the vessel wall at both day 1 and day 2 (Figure 4D and Supplemental Figure 9). These results suggest that FAK promotes tumor cell survival upon arrest in the capillary bed of the lung and is necessary for extravasation into the parenchyma of the organ.

Mammary tumorigenesis requires the Cas-binding motif of FAK. To gain insight into the signaling mechanisms through which FAK promotes tumor cell proliferation, survival, and invasion, tumor cells derived from MMTV-PyMT;FAK^{fl/fl} mice were infected with adenoviral Cre or a control virus and then reconstituted with wild-type FAK or mutants of FAK lacking defined signaling activities (Figure 5A). As anticipated, FAK-null cells displayed a proliferative and invasive deficiency and a propensity to undergo anoikis (Figure 5, B–D). Whereas reintroduction of wild-type FAK rescued tumor cell proliferation, survival, and invasion to a significant extent, FAK-K454R and FAK-Y397F did not restore these cellular functions (Figure 5, B–D), in agreement with the observation that FAK's kinase activity and autophosphorylation at Y397 are required for tumorigenicity upon orthotopic injection in the mammary fat pad (Figure 3, G–I). Notably, a double alanine substitu-

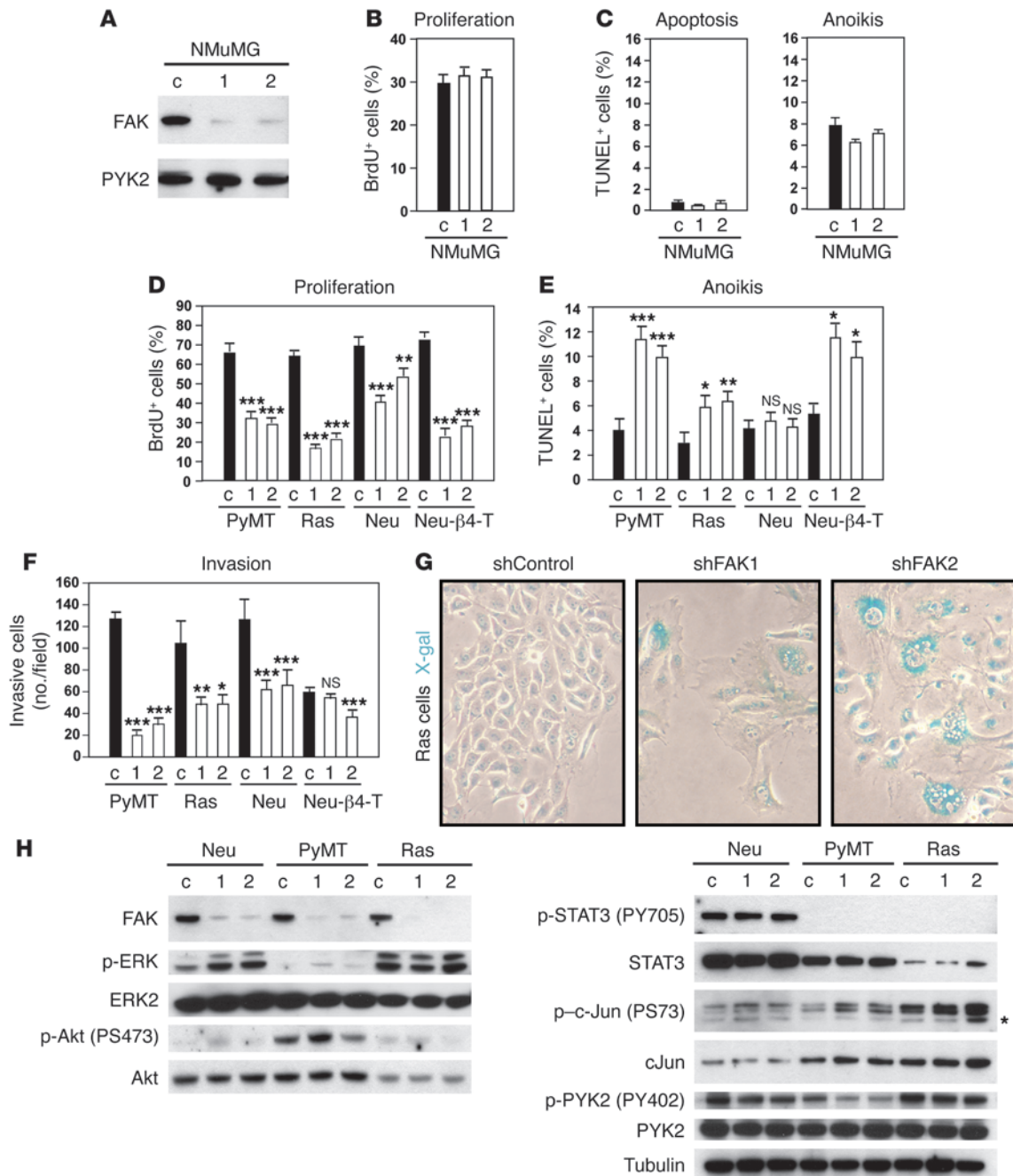


Figure 6

FAK promotes Ras-mediated mammary tumorigenesis and cooperates with integrin β4 to sustain ErbB2-mediated tumorigenesis. (A–C) Normal murine mammary gland (NMuMG) cells were transduced with empty vector (c) or vectors encoding shRNAs targeting murine FAK (1, 2) and subjected to immunoblotting (A); BrdU incorporation assay (B); and cultured under standard conditions (left) or resuspended for 8 hours (right) and subjected to TUNEL assay (C). (D–H) PyMT-, Ras-, and Neu-transformed mammary tumor cells expressing wild-type β4 (Neu) or signaling-defective β4 (Neu-β4-1355T) were transduced with empty vector or vectors encoding shRNAs targeting murine FAK (1, 2) and subjected to BrdU incorporation assay (D); cultured for 6 hours and subjected to TUNEL assay (E); or subjected to Matrigel invasion assay for 8 hours (F). Ras-transformed cells transduced with the indicated viruses were stained with X-gal (blue) (G). Original magnification, ×100. (H) Control and FAK-silenced tumor cells were subjected to immunoblotting; the asterisk indicates JunD phosphorylated at Ser100. Graphs indicate mean values (±SEM). **P* < 0.05, ***P* < 0.01, ****P* < 0.001; *n* = 3.



Table 2
Panel of breast cancer cell lines classified according to oncogenic pathway activation

Cell line	Gene cluster	ER	PR	HER2	Cancer genes
MDA-MB231 ^A	BaB	-	-	-	<i>KRAS, BRAF</i>
HS578T ^A	BaB	-	-	-	<i>HRAS</i>
BT549 ^A	BaB	-	-	-	<i>PTEN</i>
CAMA-1 ^A	Lu	+	-	-	<i>PTEN</i>
MDA-MB468 ^A	BaB	-	-	-	<i>PTEN</i>
T47D ^A	Lu	+	+	+	<i>PIK3CA</i>
MDA-MB361	Lu	+	-	+	<i>PIK3CA, HER2</i>
HCC1954	BaA	-	-	+	<i>PIK3CA, HER2</i>
BT474 ^A	Lu	+	+	+	<i>PIK3CA, HER2</i>
SK-Br3	Lu	-	-	+	<i>HER2</i>

^ACell lines sequenced at the Wellcome Trust Sanger Center (2) and found not to harbor additional mutations in cancer genes, except for those affecting the p53 or Rb regulatory circuits. Gene cluster, hormone receptor status, and HER2 amplification data are from ref. 42. PR, progesterone receptor.

tion of P712 and P713, which mediates FAK’s interaction with the SH3 domain of p130^{Cas} (41), suppressed FAK’s ability to promote tumor cell proliferation, survival, and invasion (Figure 5, B–D). By contrast, phenylalanine permutations at 2 major Src phosphorylation sites in FAK — Y863, which mediates association of FAK with integrin $\alpha\beta 5$ and VEGFR in endothelial cells, or Y926, which has been implicated in recruitment of Grb2/SOS and Ras signaling — did not debilitate FAK (Figure 5, B–D). These results suggest that FAK sustains the core functions that underlie tumorigenesis by enabling Src-mediated phosphorylation of p130^{Cas}. In accordance with this model, expression of a dominant negative form of p130^{Cas} (Cas Δ SD) inhibited the ability of FAK-proficient tumor cells to proliferate in vitro (Figure 5E).

Deletion of FAK does not affect normal mammary epithelial cells but inhibits those transformed by PyMT, Ras, and Neu. The observation that deletion of FAK does not affect postnatal development of the mammary gland but is necessary for PyMT-mediated tumorigenesis suggests that FAK exerts a specific role in tumor initiation and maintenance. To further examine this hypothesis, normal murine mammary gland (NMuMG) cells were infected with lentiviruses encoding shRNAs targeting FAK (Figure 6A). Interestingly, knockdown of FAK did not affect the ability of these cells to proliferate (Figure 6B). In addition, FAK silencing did not induce them to undergo apoptosis under standard culture conditions or sensitize them to anoikis (Figure 6C). These observations suggest that normal mammary epithelial cells are not dependent on FAK signaling for their survival or proliferation.

To examine whether the requirement for FAK during mammary tumorigenesis is oncogene specific, we examined tumor cell lines isolated from MMTV-*PyMT*, MMTV-*Neu*, and MMTV-*Ras* mice. Whereas the *PyMT*- and *Ras*-transformed cells displayed substantially elevated FAK activity as compared with normal mammary epithelial cells, the *Neu*-transformed cells exhibited modestly elevated FAK activity (Supplemental Figure 5, D and E). Treatment with serum-derived growth factors did not increase FAK activity in *PyMT*-transformed cells. However, when the 3 types of mammary tumor cells were placed in suspension, FAK activity declined substantially in all of them (Supplemental Figure 5E), indicating that integrin ligation is required for efficient activation of FAK

in cells transformed by various oncogenes. These results suggest that matrix adhesion is the major contributor to FAK activation in mammary tumor cells transformed by distinct oncogenes.

To compare the effect of loss of FAK in cells transformed by various oncogenes, we infected *Neu*-, *Ras*-, and *PyMT*-transformed mammary tumor cells with lentiviruses encoding shRNAs targeting FAK. As shown in Supplemental Figure 10, expression of 2 independent shRNAs suppressed expression of FAK in the 3 lines. FAK silencing suppressed tumor cell proliferation and invasion in *Ras*- and *PyMT*-transformed cells, but it inhibited these processes more modestly in *Neu*-transformed cells (Figure 6, D and F). In addition, loss of FAK sensitized *PyMT*-transformed cells and, to a smaller degree, *Ras*-transformed cells to anoikis, but it did not exert this effect in *Neu*-transformed cells (Figure 6E). Interestingly, mammary tumor cells transformed by *Ras*, but not those transformed by other oncogenes, acquired a very flat morphology upon knockdown of FAK. X-gal staining for senescence-associated acidic β -galactosidase activity suggested that a large fraction of *Ras*-transformed cells had become senescent (Figure 6G). Thus, knockdown of FAK suppresses invasion and induces senescence in *Ras*-transformed cells, but it exerts more moderate effects in *Neu*-transformed cells. The moderate effects of FAK silencing in *Neu*-transformed cells cannot be attributed to compensatory upregulation of PYK2, as knockdown of FAK does not increase the levels or activation of PYK2 in these or the other cells (Figure 6H).

We reasoned that knockdown of FAK inhibits *Neu*-transformed cells moderately because they are sustained by integrin $\beta 4$ signaling (8). To test this hypothesis, we knocked down FAK in *Neu*- $\beta 4$ -1355T cells, which carry a targeted deletion of the $\beta 4$ signaling domain (Supplemental Figure 10). FAK silencing induced growth arrest in *Neu*- $\beta 4$ -1355T cells and sensitized them to anoikis (Figure 6, D and E), suggesting that FAK and $\beta 4$ signaling cooperate to promote cell survival and proliferation in *Neu*-transformed cells. In agreement with the observation that $\beta 4$ signaling promotes disassembly of cell-to-cell junctions and induces scattering in *Neu*-transformed cells (8), the *Neu*- $\beta 4$ -1355T cells displayed reduced invasive ability in vitro (Figure 6F). Knockdown of FAK did not exert an additional inhibitory effect in these cells (Figure 6F), in agreement with the hypothesis that disruption of epithelial adhesion is a prerequisite for invasion. Finally, silencing of FAK did not alter the ability of *Neu*-transformed cells expressing wild-type $\beta 4$ to form orthotopic tumors in immunocompromised mice. However, it inhibited the tumorigenic potential of *Neu*- $\beta 4$ -1355T cells, which express a signaling-defective form of $\beta 4$ (Supplemental Figure 11). Taken together, these results indicate that FAK is necessary to maintain the transformed phenotype of *PyMT*- and *Ras*-transformed cells and it cooperates with $\beta 4$ to sustain *Neu*-mediated transformation.

FAK silencing does not suppress oncogene signaling. To further examine the signaling mechanisms underlying the effect of FAK on mammary tumorigenesis, control and FAK-silenced tumor cells were subjected to immunoblotting with various phospho-specific antibodies. As anticipated, Akt was activated in *PyMT*-transformed cells to a higher extent than in *Ras*- or *Neu*-transformed cells. By contrast, ERK was activated in *Ras*- and *Neu*-transformed cells to a higher level than in *PyMT*-transformed cells (Figure 6H). Interestingly, knockdown of FAK did not reduce activation of Akt or ERK in the 3 lines (Figure 6H). In addition, it did not inhibit activation of STAT3 and JNK-mediated phosphorylation of c-Jun (Figure 6H), which are both dependent on the $\beta 4$ integrin (8), or reduce NF- κ B signaling (data not shown). Collectively, these results sug-

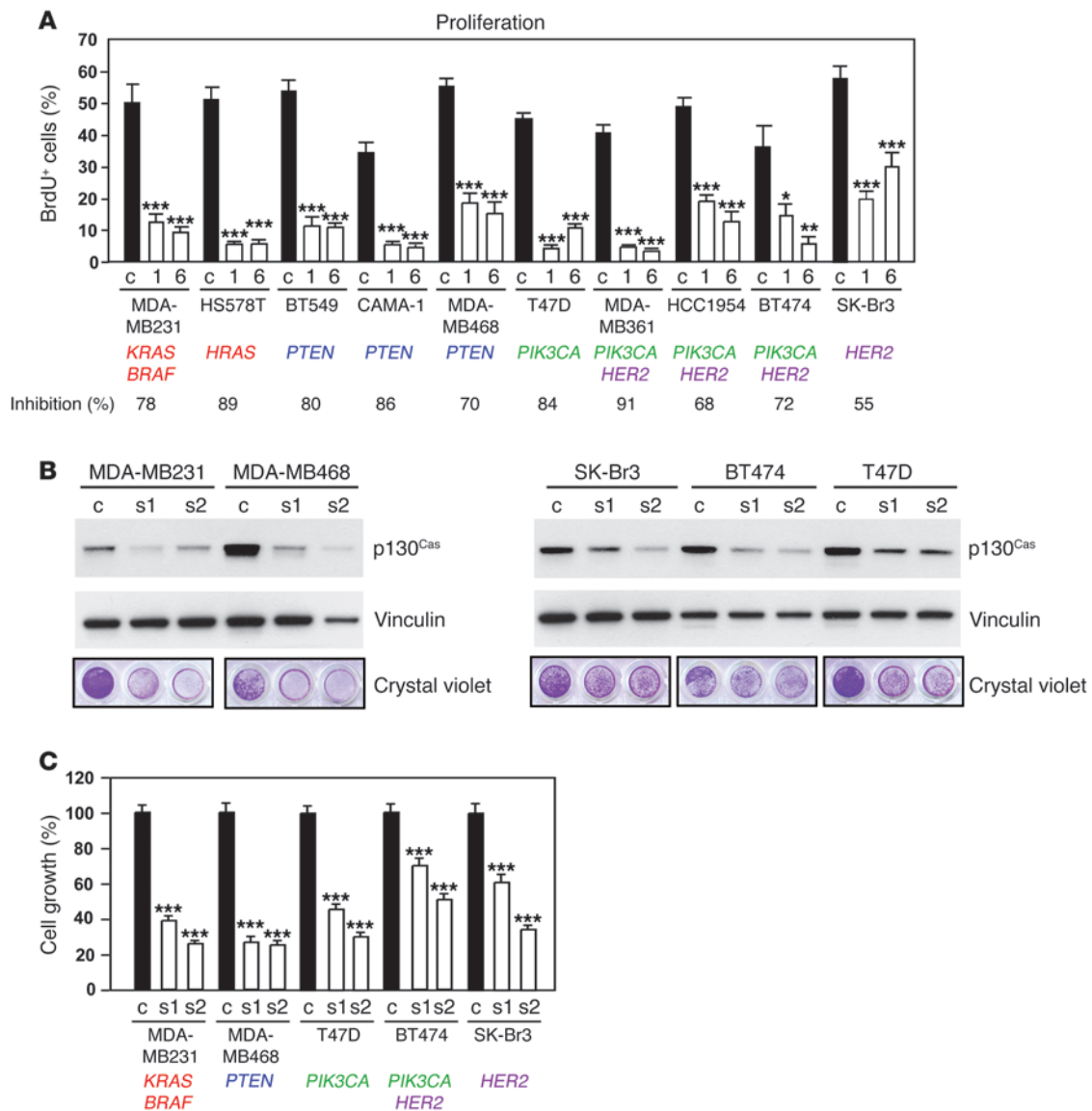


Figure 7

FAK signaling through p130^{Cas} sustains human breast cancer cells carrying clinically prevalent oncogenic mutations. **(A)** The indicated human breast cancer cells were infected with control virus or shRNAs 1 and 6 targeting FAK, synchronized in G₀, and incubated in the presence of BrdU in complete medium for 24 hours. The graph indicates the percentage of BrdU⁺ cells (±SEM). *n* = 3. Oncogenic mutations and mean percentage of inhibition after FAK silencing are indicated below. **(B)** Cancer cells were transfected with control or siRNA oligonucleotides targeting human p130^{Cas} (s1, s2) and subjected to immunoblotting or seeded in microtiter wells, cultured for 4 days in complete medium, fixed, and stained with crystal violet. **(C)** Cancer cells transfected with the indicated siRNAs were counted 4 days after seeding. Control values were normalized to 100%. ****P* < 0.001. Error bars denote SEM.

gest that loss of FAK does not affect activation of major oncogenic pathways and are consistent with the hypothesis that FAK promotes tumorigenesis, at least in part, through p130^{Cas}.

Knockdown of FAK or p130^{Cas} causes growth arrest in Ras- and PI3K-dependent human breast cancer cells. To examine the role of FAK in human breast tumorigenesis, we silenced FAK in a panel of human breast carcinoma cells carrying clinically relevant oncogenic mutations (*RAS*, *BRAF*, *PTEN*, *PIK3CA*, *HER2*) (2) and distinctive transcriptomic profiles (42) (Table 2). A large proportion of *HER2*⁺ cell lines carried *PIK3CA* mutations, in agreement with recently reported sequence analyses on clinical specimens (3). Sequencing of all the known can-

cer genes has indicated that 10 of these cell lines do not possess additional oncogenic mutations, except for those affecting the p53 or RB pathway (indicated by the footnote in Table 2; ref. 42).

Infection with 2 distinct shRNAs effectively suppressed expression of FAK in all the cell lines (Supplemental Figure 10). Notably, knockdown of FAK induced growth arrest in MDA-MB231 (*KRAS*, *BRAF*), HS578T (*HRAS*), BT549 (*PTEN*), CAMA-1 (*PTEN*), T47D (*PIK3CA*), and MDA-MB361 cells (*PIK3CA*, *HER2*), and it inhibited cell proliferation to a significant extent in MDA-MB468 (*PTEN*), HCC1954 (*HER2*, *PIK3CA*), BT474 (*HER2*, *PIK3CA*), and SK-Br3 cells (*HER2*) (Figure 7A). Interestingly, the MDA-MB361 cells, which

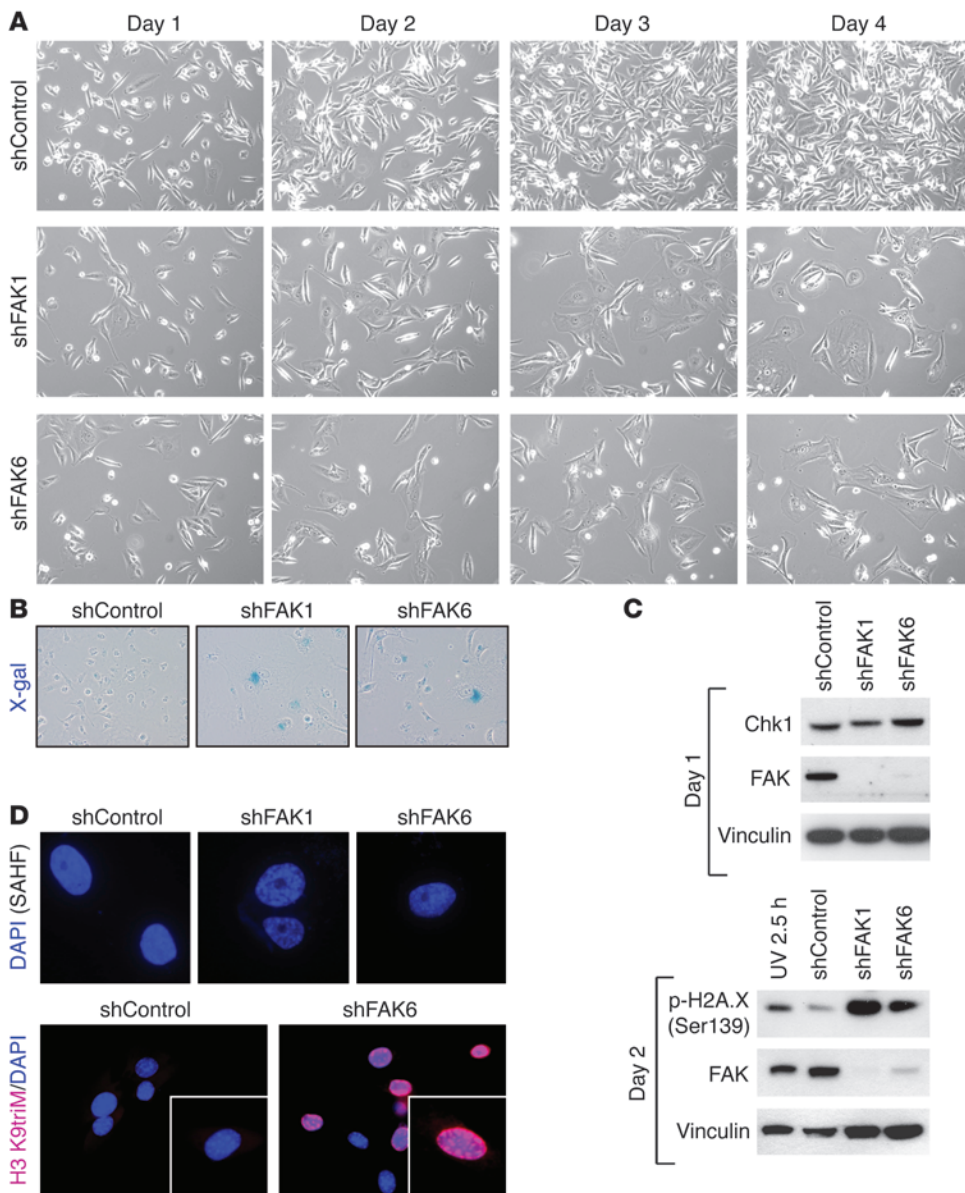


Figure 8
 Loss of FAK induces senescence in tumor cells transformed by Ras. (A–D) MDA-MB231 cells were transduced with control virus or vectors encoding shRNAs targeting FAK, cultured over a period of 4 days, and photographed at the indicated times (A; original magnification, ×100); stained with X-gal on day 4 (B; original magnification, ×100); subjected to immunoblotting with the indicated antibodies (C); or stained with DAPI alone (top) or antibodies against trimethylated H3 K9 (H3 K9triM), followed by counterstaining with DAPI (bottom) to visualize SAHF (D; original magnification, ×630; ×1,260 (insets)).

undergo growth arrest upon silencing of FAK, express low levels of ErbB2, whereas the HCC1954, BT474, and SK-Br3 cells, which are inhibited to a lesser degree, express high levels of ErbB2 (Supplemental Figure 13). These results indicate that knockdown of FAK exerts a profound inhibitory effect in breast cancer cells carrying oncogenic mutations that operate in the cytoplasm to dysregulate Ras or PI3K signaling, but it exerts a moderate inhibitory effect in breast cancer cells expressing elevated levels of ErbB2, consistent with the hypothesis that joint integrin β4–ErbB2 signaling contributes to sustaining the oncogenic behavior of these cells (Figure 6, D–F, and Supplemental Figure 11) (8). We also observed that FAK silencing inhibits proliferation but does not induce growth arrest in MDA-MB468 cells (Figure 7A), which express elevated levels of EGFR and are sensitive to EGFR kinase inhibition (43). Since the β4 integrin also combines with the EGFR and amplifies its signaling output (44), it is possible that the MDA-MB468 cells are less sensitive to the effect of FAK knockdown because they are sustained by

joint integrin β4–EGFR signaling. Together, these results suggest that FAK is required to sustain breast cancer cell transformation following hyperactivation of the PI3K or Ras signaling pathway and it enhances the proliferation of ErbB2-transformed cells.

Since mutagenesis had identified the Cas-binding motif of FAK as critical for mammary tumorigenesis (Figure 5), we examined the effect of knockdown of p130^{Cas} in 5 breast cancer cell lines representing all major oncogenic pathways operating in breast cancer. Transfection with 2 independent siRNA oligonucleotides led to significant inhibition of the expression of p130^{Cas} in all 5 lines (Figure 7B) and caused proliferative arrest in MDA-MB231 (*KRAS*, *BRAF*), MDA-MB468 (*PTEN*), and T47D cells (*PIK3CA*), but it only partially inhibited SK-Br3 (*HER2*) and BT474 cells (*HER2*, *PIK3CA*) (Figure 7, B and C). The observation that silencing of FAK and silencing of p130^{Cas} exert similar effects in 5 distinct human breast cancer cell lines suggests that FAK promotes mammary tumorigenesis by enabling Src-mediated phosphorylation of p130^{Cas}.



Silencing of FAK induces cellular senescence in breast cancer cells carrying mutant RAS. Oncogene-induced senescence operates as a barrier to neoplastic transformation in vivo. Since inactivation of FAK was able to induce Ras-transformed mouse mammary tumor cells to undergo senescent growth arrest (Figure 6G), we asked whether FAK signaling operates broadly to suppress senescence in Ras-transformed mammary epithelial cells. To address this issue, we subjected multiple human breast cancer cells carrying mutant *RAS* to silencing of FAK and monitored them over time. As shown in Figure 8A, the MDA-MB231 cells became progressively flatter and underwent complete growth arrest over a period of 4 days in culture. X-gal staining for senescence-associated β -galactosidase activity indicated that these cells had undergone senescence (Figure 8B). Similar results were obtained with HS578T and SK-Br7 cells, which also carry mutant *RAS* (Supplemental Figure 12 and data not shown). In contrast, human breast cancer cells carrying *PIK3CA* and *PTEN* mutations became round and eventually detached from the substrate, possibly because they had become apoptotic (Supplemental Figure 12). While these cells could not be further propagated, those expressing high levels of ErbB2 were affected less severely (Supplemental Figure 12). These results suggest that FAK signaling operates to prevent Ras-induced senescence in human breast cancer cells.

Oncogenic *RAS* and *BRAF* are thought to induce senescence predominantly through aberrant DNA replication, which causes a DNA damage response (45). In response to DNA damage, the ATM/ATR kinases activate the checkpoint kinases Chk1 and Chk2, thereby promoting assembly of multiprotein complexes at DNA damage sites. Phosphorylation of histone H2A.X is thought to contribute to stabilization of these complexes at DNA damage sites (45). To determine whether loss of FAK causes senescence by allowing activation of a DNA damage response, we examined the activation of Chk1 and phosphorylation of H2A.X in FAK-silenced MDA-MB231 cells. As shown in Figure 8C, 1 day after infection with shRNAs targeting FAK, MDA-MB231 cells displayed a decrease in electrophoretic mobility of Chk1, consistent with phosphorylation and activation of this kinase. One day later, H2A.X became robustly phosphorylated at S139, suggesting that inactivation of FAK allows activation of a DNA damage response in Ras-transformed cells (Figure 8C).

Ultimately, cellular senescence requires alteration of gene expression, in particular repression of E2F target cell cycle genes. Reorganization of chromatin into discrete foci, termed senescence-associated heterochromatic foci (SAHF), contributes to silencing of E2F-dependent genes during senescence (45). As shown in Figure 8D, DAPI staining indicated that knockdown of FAK causes the appearance of heterochromatic foci in MDA-MB231 cells. These foci are excluded from nucleoli, which renders them more prominent. SAHF are sites of gene silencing and are therefore marked by methylation of histone H3 at K9. To examine whether the heterochromatic foci detected in FAK-silenced MDA-MB231 cells were indeed SAHF, we used staining with antibodies against trimethylated H3 K9. As shown in Figure 8D, the foci reacted strongly with these antibodies. These results indicate that loss of FAK induces a senescent growth arrest program in Ras-transformed breast cancer cells.

Discussion

Our study reveals that *FAK* is amplified and overexpressed in a large fraction of primary human breast cancers. Elimination of FAK does not obviously affect mammary gland development, but it suppresses tumor initiation and progression in the PyMT model of breast cancer. In cell culture, FAK does not appear to be neces-

sary for normal cell survival and proliferation. However, it supports Ras- and PI3K-dependent neoplastic transformation by orchestrating multiple core functions, including proliferation, survival, and avoidance of senescence. In addition, FAK is necessary for tumor invasion and metastasis. We conclude that FAK exerts critical functions at multiple steps of mammary tumorigenesis. The exquisite dependency of Ras- and PI3K-transformed mammary tumor cells on FAK signaling has broad biological implications and identifies a vulnerability that could be exploited therapeutically.

The gene encoding human FAK resides distal to *MYC* at 8q23 within a chromosomal segment that is characterized by frequent aberrations in breast cancer (31). FISH analysis of 79 primary tumors collected at MSKCC has revealed that *FAK* is commonly amplified in breast cancer: 50% of the samples examined were found to contain copy number gains and 10% contained high-level amplifications. Amplification at the *FAK* locus correlated with increased expression of FAK but not *MYC* in these samples, suggesting that FAK is capable of driving expansion of the distal amplicon detected at 8q23 (32). Two lines of evidence suggest that overexpression of FAK is of clinical significance. First, elevated expression of FAK is inversely correlated with metastasis-free survival in the large cohort of patients from the NKI dataset. Second, multivariate analysis indicates that elevated FAK is an independent predictor of poor outcome and it outperforms many commonly used clinical parameters, such as lymph node involvement, ER negativity, and poor differentiation, as assessed by histology. These findings indicate that *FAK* is frequently amplified in breast cancer and suggest that FAK overexpression negatively affects the clinical course of the disease.

Conditional deletion of FAK does not obviously affect mammary gland development, but it suppresses tumor initiation and progression in the PyMT model of breast cancer. Strikingly, virtually all the adenocarcinomas that nonetheless arose in the mutant background were composed of cells expressing FAK, and in mice bred into the Rosa26 reporter (*Rosa26R*) strain, adenocarcinomas were found to have originated from cells that had escaped Cre-mediated recombination of *FAK*. To determine whether FAK is necessary for tumor initiation, we have focused on MIN lesions, which constitute the first morphologically recognizable neoplastic lesions arising in the mammary gland (39). We found that greater than 80% of the MIN lesions arising in FAK mutant mice had originated from cells that had escaped Cre-mediated recombination. In fact, even the earliest MIN lesions budding out of otherwise seemingly normal ducts or the smallest intraductal lesions consisted almost exclusively of cells expressing FAK but not Cre. These results document a stringent requirement for FAK during mammary tumor initiation.

Muller and colleagues have argued instead that deletion of FAK does not affect PyMT-mediated transformation of the mammary gland (26). Although they have not estimated the percentage of MIN lesions lacking FAK in their *MMTV-Cre;FAK^{fl/fl}* mice, they have noticed several early adenomas lacking FAK in these mice. How do we explain this apparent discrepancy? We believe that the major difference between our compound mice and theirs lies in the efficiency of Cre-mediated deletion. Since the *Cre* transgene we have employed deletes in more than 95% of mammary epithelial cells, it is more likely that this transgene is activated early in the developmental hierarchy that gives rise to differentiated progeny in the mammary gland. In other words, we suspect that our *Cre* transgene is activated and thereby deletes *FAK* in stem or progenitor cells. In contrast, their transgene may not be activated in these cells, allowing for their transformation. Since tumor progenitor cells are estimated



to constitute a minority of cells in tumors (46), the bulk of more-differentiated cells in their early adenomas are likely to have undergone *Cre*-mediated deletion of *FAK* and thereby fail to express the protein. Yet they may have originated from progenitor cells expressing *FAK*.

To examine the cellular mechanisms through which *FAK* supports mammary oncogenesis, we used genetic methods to inactivate *FAK* in mouse mammary tumor cells transformed by *PyMT*, activated *Ras*, or *Neu*. Provocatively, loss of *FAK* caused growth arrest followed by apoptosis in tumor cells transformed by *PyMT* and senescence in those transformed by activated *Ras*. Although elimination of *FAK* exerted a more moderate effect in *ErbB2*-transformed cells, it induced those carrying a deletion of the $\beta 4$ signaling domain to undergo growth arrest and apoptosis, suggesting that *FAK* cooperates with the $\beta 4$ integrin to sustain these cancer cells. Similarly, inactivation of *FAK* induced growth arrest followed by apoptosis in human breast cancer cells carrying mutant *PIK3CA* or *PTEN*, induced senescence in those harboring mutant *RAS*, and exerted more moderate inhibitory effects in those carrying *HER2* amplifications. These results suggest that *FAK* is required to maintain neoplastic transformation in mammary tumor cells carrying oncogenic mutations that potently activate *Ras* or *PI3K* and that it cooperates with the $\beta 4$ integrin to promote *ErbB2*-mediated tumorigenesis.

To examine the role of *FAK* in mammary tumor invasion and metastasis, we used a lung colonization assay. Bioluminescence imaging indicated that loss of *FAK* completely suppresses metastasis in this assay. Confocal microscopy followed by 3D reconstruction revealed that *FAK*-deficient mammary tumor cells are not metastatic for 2 major reasons: they survive poorly in the microvascular compartment of the lung, and they are unable to extravasate into the parenchyma of the organ. In agreement with this conclusion, we observed that loss of *FAK* increases sensitivity to anoikis and inhibits Matrigel invasion in mammary tumor cells transformed by various oncogenes. Together with the correlation between *FAK* expression and poor metastasis-free survival observed in the *NKI* dataset, these results suggest that *FAK* plays a broad prometastatic role in breast cancer.

What is the mechanism through which *FAK* promotes mammary tumorigenesis? The *FAK*/*SFK* complex has multiple substrates (13, 14), but our mutational analysis suggests that the ability of *FAK* to support oncogenesis specifically depends on the integrity of *Pro712* and *Pro713*, which mediate *FAK*'s interaction with the *SH3* domain of *p130^{Cas}* (41). In addition, knockdown of *p130^{Cas}* phenocopies the effect of loss of *FAK* in human breast cancer cell lines carrying multiple, distinct, clinically relevant oncogenic mutations, suggesting that *FAK* supports mammary tumorigenesis largely through *p130^{Cas}*. Interestingly, *p130^{Cas}* is necessary for morphological transformation of fibroblasts by the viral oncogene *Src* (47), and overexpression of *p130^{Cas}* promotes hyperplasia and accelerates *ErbB2*-mediated tumorigenesis in the mammary gland of transgenic mice (48).

Whereas the mechanisms through which *p130^{Cas}* regulates cell migration and tumor cell invasion are understood to a significant detail, those which may enable *p130^{Cas}* to promote cell survival and proliferation and thereby tumorigenicity are not clear (41). It is intriguing, however, that a major target-effector of *p130^{Cas}*, the adaptor protein *Crk*, can transform fibroblasts *in vitro* when it is deregulated by viral fusion or a mutation that impairs auto-inhibition (49). In addition, *Crk* can interact with several potentially pro-oncogenic proteins, including *c-Abl*, *SOS*, and *JNK* (41). Adding more complexity, the substrate domain of *p130^{Cas}* undergoes mechanical extension and is primed for phosphorylation by *FAK*/*SFK* in response to reinforcement of integrin-cytoskeletal linkages (50). Since mammary

tumor cells acquire a contractile phenotype upon adhering to a fibrotic, rigid stroma (51), it is possible that *p130^{Cas}* undergoes extension and multisite phosphorylation under these conditions, resulting in enhanced signaling. Together, these observations suggest the possibility that the *FAK*/*Src* complex and its target-effector *p130^{Cas}* are integral components of the mechanoregulatory circuit that controls tensional homeostasis in the mammary gland (51, 52) and that amplification and overexpression of *FAK* contributes to disruption of this regulatory circuit during mammary tumorigenesis. Our results, however, do not exclude the possibility that in addition to *p130^{Cas}*, other *FAK*/*SFK* substrates contribute to mammary oncogenesis.

The observation that loss of *FAK* allows activation of a DNA damage response followed by induction of senescence in cells transformed by activated *RAS* is unexpected. Hyperactivation of *Ras* signaling causes senescence in primary fibroblasts and epithelial cells *in vitro* and in transgenic models of various cancers, including breast cancer (53), but loss of *p53* or *Rb* function can counteract this effect of *Ras* to allow transformation. Since inactivation of *FAK* also induces senescence in *MDA-MB231* cells, which carry mutant *P53* and *CDKN2*, *FAK* does not appear to oppose senescence by inhibiting *p53* or *p16* function. The observation that activated *Ras* signaling also induces senescence independently of *Rb* or *p53* in normal mammary epithelial cells (54) suggests that loss of *FAK* allows reactivation of a *Ras*-dependent senescence program. The ability of *FAK* to prevent senescence in cells fully transformed by mutant *RAS* suggests that these cells do not conclusively avert the risk of undergoing senescence through the acquisition of additional oncogenic mutations, but they require continuous *FAK* signaling to maintain their replicative potential.

Our findings indicate that *FAK* is an integral and necessary component in the network of signaling interactions that initiate and support mammary tumorigenesis. The observation that *FAK* is frequently amplified in human breast cancer suggests the possibility that *FAK* may function as a classical oncogene in mammary epithelium. Formal proof that this is the case will require demonstration that overexpression of *FAK* can initiate tumorigenesis in this tissue *in vivo*. Alternatively, it is possible that *FAK* is a potent, general modifier of oncogenesis, akin to the heat shock protein *HSP90* and the transcription factor heat shock factor 1 (*HSF1*) (55). In either case, the requirement for *FAK* illustrated by our results suggests new therapeutic opportunities. In particular, the observation that loss of *FAK* does not affect the ability of normal mammary epithelial cells to survive and proliferate, both *in vitro* and *in vivo*, but exerts striking inhibitory effects in mammary tumor cells carrying oncogenic mutations, which activate *Ras* or *PI3K*, suggest that these cells may be addicted to *FAK* signaling, as they are to oncogene signaling (1). Since *FAK* appears to operate largely in parallel with classical oncogenic signaling, combined inhibition of *FAK* and either *PI3K* or *Ras* signaling may exhibit broad therapeutic efficacy in breast cancer.

Methods

Cell culture, antibodies, constructs, and other reagents. See Supplemental Methods.

Tumorigenesis and metastasis studies. *FAK^{β/β}* mice (17) were crossed to *MMTV-Cre* mice (transgenic line D) (34) and then bred to *MMTV-PyMT* mice (gift from T. Ludwig, Institute for Cancer Genetics, Columbia University, New York, New York, USA) (56). *R26R* mice were obtained from The Jackson Laboratory (57). Tumorigenesis studies were performed on littermates from crosses among *FAK^{β/β};MMTV-Cre;MMTV-PyMT* mice. Tumors were detected by palpation when they reached 3–4 mm in diameter. For orthotopic transplantation, 2×10^5 or 2.5×10^5 cells were suspended in 50 μ l of growth



factor-reduced Matrigel diluted 1:1 in PBS and injected into the surgically exposed fat pad of mammary gland 4. Tumor dimensions were measured by using a caliper. For experimental metastasis studies, cells were transduced with the TGL vector (40) and injected at 1×10^6 in 100 μ l of PBS in the tail vein of NOD/SCID mice. Animals were imaged in an IVIS 100 chamber (Caliper Life Sciences), and data were recorded using Living Image software. All mouse studies were conducted in accordance with protocols approved by the Institutional Animal Care and Use Committee of MSKCC.

Immunostaining. Paraffin-embedded sections were subjected to immunohistochemistry with the ImmunoCruz Staining System (Santa Cruz Biotechnology Inc.) and to immunofluorescence staining using the automated Leica staining system (see Supplemental Methods). Probes for FISH to *FAK* and the centromere of chromosome 8 were generated at the Molecular Cytogenetics Core Facility of MSKCC, conjugated to FITC (for *FAK*) or TRITC (centromere 8), and hybridized to tissue microarrays. FISH results were scored according to Walker et al. (58). Representative images of each tumor section were taken using Z stacking and Metafer software (Metasystems). To generate antisense and sense probes for DIG labeling, a murine *FAK* cDNA was transcribed with the T3 or the T7 polymerase in the presence of DIG labeling mix (Roche) (see Supplemental Methods). The probes were then hybridized to paraffin-embedded sections using an automated system and subsequently counterstained with eosin. To improve confocal analysis of tumor cells extravasating in the lungs, we incubated TGL-transduced cells with 5 μ M Oregon green 488 (BD) in DMSO for 1.5 hours at 37°C prior to tail vein injection. Lung tissue was inflated with 1.5 ml ice-cold paraformaldehyde, fixed overnight, and embedded in O.C.T., and 50- μ m sections were cut on a Leica microtome. Sections were stained with anti-PECAM-1 by using the Tyramide Signal Amplification Kit from Invitrogen.

Whole-mount preparation. Mammary glands were mounted on slides, dried overnight, and fixed with acetone. Samples were immersed in Harris's modified hematoxylin, destained with 1% HCl in ethanol, and fixed briefly in 0.02% ammonium hydroxide. Tissues were cleared by immersion in xylene and mounted in Permount.

In situ β -galactosidase assay. Freshly dissected mammary glands and whole-mount preparations were fixed in 4% paraformaldehyde on ice for 2 hours. The tissues were then washed 3 times in washing buffer (PBS containing 2 mM MgCl₂, 5 mM EGTA, 0.01% sodium deoxycholate, 0.02% NP-40) and stained in fresh X-gal staining solution [PBS containing 2 mM MgCl₂, 5 mM EGTA, 0.01% sodium deoxycholate, 0.02% NP-40, 5 mM K₃Fe(CN)₆, 5 mM K₄Fe(CN)₆, 1 mg/ml X-gal] overnight at 37°C. After washing in PBS, tissues were mounted in Permount. For sectioning, tissues were embedded in paraffin, cut, and counterstained with eosin. β -Galactosidase assays on cells in culture were performed by using the Senescence β -galactosidase Staining Kit from Cell Signaling Technology.

Isolation of primary cells. Tumors were dissociated by incubation with 1.25 mg/ml collagenase type III and 1 mg/ml hyaluronidase (Worthington Biochemical Corp.) for 2 hours. Cells were spun down and resuspended in 0.25% trypsin for 10 minutes at 37°C. They were then spun down again and resuspended in 20 U/ml DNase I for 10 minutes at 37°C. After washing with 5% serum in PBS, cells were passed through a 70- μ m cell strainer and plated on collagen I (20 μ g/ml) in complete medium. Primary tumor cells underwent growth arrest after 3–4 passages in culture, presumably because of insufficient activity of the MMTV promoter in vitro. The cells were therefore transduced with pBabe-PyMT and further selected in hygromycin. Non-transformed primary mammary epithelial cells were dissociated from fat pads as described above, but they were not passed through a cell strainer.

Retroviral and lentiviral stocks. Retroviral expression vectors were transfected into 293GPG packaging cells (59). To generate lentiviral vectors, we cotransfected 293FT cells (Invitrogen) with the following 3 plasmids: the short hairpin encoding vector (pLKO1 from Open Biosystems, TRC Consortium), the

packaging construct (pHR-CMV-dR8.2), and the envelope plasmid (pCMV-VSVG). Viral stocks were filtered through a 45 μ m filter and concentrated by centrifugation at 50,000 g at 4°C for 2 hours. Experimental manipulation of cells was typically done at 72 hours after infection.

Biochemical methods. For immunoblotting, cells were lysed in 1% NP-40 buffer (50 mM HEPES pH 7.4, 1% NP-40, 150 mM NaCl, 10% glycerol, 1 mM EGTA, 1 mM EDTA, 25 mM NaF, 1 mM Na vanadate, and protease inhibitors). Fresh tumor tissues were flash-frozen in liquid nitrogen, crushed into powder, and then suspended in lysis buffer.

Invasion assay. Cells (1×10^5) were counted using Trypan blue reagent (Sigma-Aldrich), normalized for the number of viable cells, and placed in SFM on Transwell inserts coated with 2 μ g Matrigel. Following incubation in 24-well plates containing complete medium for 6–8 hours, inserts were fixed with 4% paraformaldehyde for 10 minutes at room temperature and stained with crystal violet.

Anoikis assay. Cells were resuspended in complete medium containing 0.5% methylcellulose and 1% BSA for at least 6 hours at 37°C, attached to a polylysine-coated chamber slide for 10 minutes, and subjected to TUNEL assay (Roche).

BrdU assay. Cells were cultured on collagen I, deprived of growth factors for 24 to 36 hours, incubated in the presence of BrdU in either SFM or complete medium for 24 hours, and subjected to anti-BrdU staining (Roche).

Statistics. Kaplan-Meier curves were prepared by using Prism software (Prism Software Corp.). *P* values were generated using Student's *t* test (unpaired, 2-tailed); a *P* value less than 0.05 was considered significant. Multivariate analysis was performed using the Cox proportional hazards model (R programming language).

Note added in proof. Keely and colleagues have reported that deletion of *FAK* retards but does not prevent tumor formation in the PyMT model (60). Inefficient Cre-mediated deletion of *FAK* in tumor progenitor cells may explain the formation of *FAK*-expressing tumors in this study, as we have discussed herein with regard to the study by the Muller group (26).

Acknowledgments

We thank L. Chin for vectors encoding shRNAs against murine *FAK* (shFAK1 and shFAK2; original source: TRC Consortium); E. Marcantonio and Y.C. Du for cDNA constructs; T. Ludwig for MMTV-PyMT mice; P. Leder for the SH1.1 cell line; N. Rosen for reagents; the Molecular Cytology and Molecular Cytogenetics Core Facilities of MSKCC for technical help; G.P. Gupta for discussions and help with statistical analyses; and A. Olshen and members of the Giancotti laboratory for discussions. This study was supported by NIH awards R37 CA58976 (to F.G. Giancotti), R01 NS199090 (to L.F. Reichardt), and P30 CA08748 (to MSKCC).

Received for publication August 14, 2008, and accepted in revised form December 3, 2008.

Address correspondence to: Filippo G. Giancotti, Memorial Sloan-Kettering Cancer Center, 1275 York Avenue, Box 216, New York, New York 10065, USA. Phone: (212) 639-7333; Fax: (212) 794-6236; E-mail: f-giancotti@ski.mskcc.org. Or to: Yuliya Pylyayeva, Department of Biochemistry, NYU School of Medicine, 550 First Avenue, MSB 398, New York, NY 10016, USA. Phone: (212) 263-2937; Fax: (212) 263-8166; E-mail: pylayy01@nyumc.org.

Yuliya Pylyayeva's present address is: Department of Biochemistry, NYU School of Medicine, New York, New York, USA.

William Gerald is deceased.



1. Weinstein, I.B. 2002. Cancer. Addiction to oncogenes – the Achilles heel of cancer. *Science*. **297**:63–64.
2. Forbes, S., et al. 2006. Cosmic 2005. *Br. J. Cancer*. **94**:318–322.
3. Saal, L.H., et al. 2005. PIK3CA mutations correlate with hormone receptors, node metastasis, and ERBB2, and are mutually exclusive with PTEN loss in human breast carcinoma. *Cancer Res*. **65**:2554–2559.
4. Carpten, J.D., et al. 2007. A transforming mutation in the pleckstrin homology domain of AKT1 in cancer. *Nature*. **448**:439–444.
5. Elenbaas, B., et al. 2001. Human breast cancer cells generated by oncogenic transformation of primary mammary epithelial cells. *Genes Dev*. **15**:50–65.
6. Zhao, J.J., et al. 2005. The oncogenic properties of mutant p110alpha and p110beta phosphatidylinositol 3-kinases in human mammary epithelial cells. *Proc. Natl. Acad. Sci. U. S. A.* **102**:18443–18448.
7. Giancotti, F.G., and Taronè, G. 2003. Positional control of cell fate through joint integrin/receptor protein kinase signaling. *Annu. Rev. Cell Dev. Biol.* **19**:173–206.
8. Guo, W., et al. 2006. Beta 4 integrin amplifies ErbB2 signaling to promote mammary tumorigenesis. *Cell*. **126**:489–502.
9. Schwartz, M.A. 1997. Integrins, oncogenes, and anchorage independence. *J. Cell Biol.* **139**:575–578.
10. Hood, J.D., and Cheresch, D.A. 2002. Role of integrins in cell invasion and migration. *Nat. Rev. Cancer*. **2**:91–100.
11. Guo, W., and Giancotti, F.G. 2004. Integrin signaling during tumour progression. *Nat. Rev. Mol. Cell Biol.* **5**:816–826.
12. White, D.E., et al. 2004. Targeted disruption of beta1-integrin in a transgenic mouse model of human breast cancer reveals an essential role in mammary tumor induction. *Cancer Cell*. **6**:159–170.
13. Parsons, J.T. 2003. Focal adhesion kinase: the first ten years. *J. Cell. Sci.* **116**:1409–1416.
14. Mitra, S.K., Hanson, D.A., and Schlaepfer, D.D. 2005. Focal adhesion kinase: in command and control of cell motility. *Nat. Rev. Mol. Cell Biol.* **6**:56–68.
15. Ilic, D., et al. 1995. Reduced cell motility and enhanced focal adhesion contact formation in cells from FAK-deficient mice. *Nature*. **377**:539–544.
16. Schober, M., et al. 2007. Focal adhesion kinase modulates tension signaling to control actin and focal adhesion dynamics. *J. Cell Biol.* **176**:667–680.
17. Beggs, H.E., et al. 2003. FAK deficiency in cells contributing to the basal lamina results in cortical abnormalities resembling congenital muscular dystrophies. *Neuron*. **40**:501–514.
18. Shen, T.L., et al. 2005. Conditional knockout of focal adhesion kinase in endothelial cells reveals its role in angiogenesis and vascular development in late embryogenesis. *J. Cell Biol.* **169**:941–952.
19. Lim, Y., et al. 2008. PyK2 and FAK connections to p190Rho guanine nucleotide exchange factor regulate RhoA activity, focal adhesion formation, and cell motility. *J. Cell Biol.* **180**:187–203.
20. Weis, S.M., et al. 2008. Compensatory role for Pyk2 during angiogenesis in adult mice lacking endothelial cell FAK. *J. Cell Biol.* **181**:43–50.
21. Pirone, D.M., et al. 2006. An inhibitory role for FAK in regulating proliferation: a link between limited adhesion and RhoA-ROCK signaling. *J. Cell Biol.* **174**:277–288.
22. Lim, S.T., et al. 2008. Nuclear FAK promotes cell proliferation and survival through FERM-enhanced p53 degradation. *Mol. Cell*. **29**:9–22.
23. Hauck, C.R., Hsia, D.A., Puente, X.S., Cheresch, D.A., and Schlaepfer, D.D. 2002. FRNK blocks v-Src-stimulated invasion and experimental metastases without effects on cell motility or growth. *EMBO J.* **21**:6289–6302.
24. Hsia, D.A., et al. 2003. Differential regulation of cell motility and invasion by FAK. *J. Cell Biol.* **160**:753–767.
25. McLean, G.W., et al. 2004. Specific deletion of focal adhesion kinase suppresses tumor formation and blocks malignant progression. *Genes Dev*. **18**:2998–3003.
26. Lahlou, H., et al. 2007. Mammary epithelial-specific disruption of the focal adhesion kinase blocks mammary tumor progression. *Proc. Natl. Acad. Sci. U. S. A.* **104**:20302–20307.
27. Benlimame, N., et al. 2005. FAK signaling is critical for ErbB-2/ErbB-3 receptor cooperation for oncogenic transformation and invasion. *J. Cell Biol.* **171**:505–516.
28. Mitra, S.K., Lim, S.T., Chi, A., and Schlaepfer, D.D. 2006. Intrinsic focal adhesion kinase activity controls orthotopic breast carcinoma metastasis via the regulation of urokinase plasminogen activator expression in a syngeneic tumor model. *Oncogene*. **25**:4429–4440.
29. Watermann, D.O., et al. 2005. Specific induction of pp125 focal adhesion kinase in human breast cancer. *Br. J. Cancer*. **93**:694–698.
30. Madan, R., Smolkin, M.B., Cocker, R., Fayyad, R., and Oktay, M.H. 2006. Focal adhesion proteins as markers of malignant transformation and prognostic indicators in breast carcinoma. *Hum. Pathol.* **37**:9–15.
31. Jain, A.N., et al. 2001. Quantitative analysis of chromosomal CGH in human breast tumors associates copy number abnormalities with p53 status and patient survival. *Proc. Natl. Acad. Sci. U. S. A.* **98**:7952–7957.
32. Naylor, T.L., et al. 2005. High resolution genomic analysis of sporadic breast cancer using array-based comparative genomic hybridization. *Breast Cancer Res.* **7**:R1186–R1198.
33. Chang, H.Y., et al. 2005. Robustness, scalability, and integration of a wound-response gene expression signature in predicting breast cancer survival. *Proc. Natl. Acad. Sci. U. S. A.* **102**:3738–3743.
34. Wagner, K.U., et al. 2001. Spatial and temporal expression of the Cre gene under the control of the MMTV-LTR in different lines of transgenic mice. *Transgenic Res.* **10**:545–553.
35. Klingbeil, C.K., et al. 2001. Targeting Pyk2 to beta 1-integrin-containing focal contacts rescues fibronectin-stimulated signaling and haptotactic motility defects of focal adhesion kinase-null cells. *J. Cell Biol.* **152**:97–110.
36. Nagy, T., et al. 2007. Mammary epithelial-specific deletion of the focal adhesion kinase gene leads to severe lobulo-alveolar hypoplasia and secretory immaturity of the murine mammary gland. *J. Biol. Chem.* **282**:31766–31776.
37. Lin, E.Y., et al. 2003. Progression to malignancy in the polyoma middle T oncoprotein mouse breast cancer model provides a reliable model for human diseases. *Am. J. Pathol.* **163**:2113–2126.
38. Maglione, J.E., et al. 2001. Transgenic Polyoma middle-T mice model premalignant mammary disease. *Cancer Res*. **61**:8298–8305.
39. Kourou-Mehr, H., et al. 2008. GATA-3 links tumor differentiation and dissemination in a luminal breast cancer model. *Cancer Cell*. **13**:141–152.
40. Blasberg, R.G., and Tjuvajev, J.G. 2003. Molecular-genetic imaging: current and future perspectives. *J. Clin. Invest.* **111**:1620–1629.
41. Chodniewicz, D., and Klemke, R.L. 2004. Regulation of integrin-mediated cellular responses through assembly of a CAS/Crk scaffold. *Biochim. Biophys. Acta*. **1692**:63–76.
42. Neve, R.M., et al. 2006. A collection of breast cancer cell lines for the study of functionally distinct cancer subtypes. *Cancer Cell*. **10**:515–527.
43. Konecny, G.E., et al. 2006. Activity of the dual kinase inhibitor lapatinib (GW572016) against HER-2-overexpressing and trastuzumab-treated breast cancer cells. *Cancer Res*. **66**:1630–1639.
44. Mariotti, A., et al. 2001. EGF-R signaling through Fyn kinase disrupts the function of integrin alpha-6beta4 at hemidesmosomes: role in epithelial cell migration and carcinoma invasion. *J. Cell Biol.* **155**:447–458.
45. Campisi, J., and d'Adda di Fagagna, F. 2007. Cellular senescence: when bad things happen to good cells. *Nat. Rev. Mol. Cell Biol.* **8**:729–740.
46. Reya, T., Morrison, S.J., Clarke, M.F., and Weissman, I.L. 2001. Stem cells, cancer, and cancer stem cells. *Nature*. **414**:105–111.
47. Honda, H., et al. 1998. Cardiovascular anomaly, impaired actin bundling and resistance to Src-induced transformation in mice lacking p130Cas. *Nat. Genet.* **19**:361–365.
48. Cabodi, S., et al. 2006. p130Cas as a new regulator of mammary epithelial cell proliferation, survival, and HER2-neu oncogene-dependent breast tumorigenesis. *Cancer Res*. **66**:4672–4680.
49. Feller, S.M., Ren, R., Hanafusa, H., and Baltimore, D. 1994. SH2 and SH3 domains as molecular adhesives: the interactions of Crk and Abl. *Trends Biochem. Sci.* **19**:453–458.
50. Sawada, Y., et al. 2006. Force sensing by mechanical extension of the Src family kinase substrate p130Cas. *Cell*. **127**:1015–1026.
51. Paszek, M.J., et al. 2005. Tensional homeostasis and the malignant phenotype. *Cancer Cell*. **8**:241–254.
52. Wozniak, M.A., Desai, R., Solski, P.A., Der, C.J., and Keely, P.J. 2003. ROCK-generated contractility regulates breast epithelial cell differentiation in response to the physical properties of a three-dimensional collagen matrix. *J. Cell Biol.* **163**:583–595.
53. Sarkisian, C.J., et al. 2007. Dose-dependent oncogene-induced senescence in vivo and its evasion during mammary tumorigenesis. *Nat. Cell Biol.* **9**:493–505.
54. Olsen, C.L., Gardie, B., Yaswen, P., and Stampfer, M.R. 2002. Raf-1-induced growth arrest in human mammary epithelial cells is p16-independent and is overcome in immortal cells during conversion. *Oncogene*. **21**:6328–6339.
55. Solimini, N.L., Luo, J., and Elledge, S.J. 2007. Non-oncogene addiction and the stress phenotype of cancer cells. *Cell*. **130**:986–988.
56. Guy, C.T., Cardiff, R.D., and Muller, W.J. 1992. Induction of mammary tumors by expression of polyomavirus middle T oncogene: a transgenic mouse model for metastatic disease. *Mol. Cell Biol.* **12**:954–961.
57. Soriano, P. 1999. Generalized lacZ expression with the ROSA26 Cre reporter strain. *Nat. Genet.* **21**:70–71.
58. Walker, R.A., et al. 2008. HER2 testing in the UK: further update to recommendations. *J. Clin. Pathol.* **61**:818–824.
59. Ory, D.S., Neugeboren, B.A., and Mulligan, R.C. 1996. A stable human-derived packaging cell line for production of high titer retrovirus/vesicular stomatitis virus G pseudotypes. *Proc. Natl. Acad. Sci. U. S. A.* **93**:11400–11406.
60. Provenzano, P.P., Inman, D.R., Eliceiri, K.W., Beggs, H.E., and Keely, P.J. 2008. Mammary epithelial-specific disruption of focal adhesion kinase retards tumor formation and metastasis in a transgenic mouse model of human breast cancer. *Am. J. Pathol.* **173**:1551–1565.